

ATTEYA, A.I., EL-ZONKOLY, A., ASHOUR, H.A. and ALI, D. 2025. Towards digitalized and automated substations: implementation of adaptive protection control unit and monitoring system for modern distribution networks under increased hosting capacity of distributed renewable sources. IET conference proceedings: proceedings of the 2024 International conference on electricity distribution workshop (CIRED 2024 Vienna workshop), 19-20 June 2024, Vienna, Austria, [online] 2024(5), pages 609-616. Available from: <https://doi.org/10.1049/icp.2024.2114>

# Towards digitalized and automated substations: implementation of adaptive protection control unit and monitoring system for modern distribution networks under increased hosting capacity of distributed renewable sources.

ATTEYA, A.I., EL-ZONKOLY, A., ASHOUR, H.A. and ALI, D.

2024

© The Institution of Engineering and Technology. This is the accepted manuscript version of the above paper. The version of record will eventually be available on IEEE Xplore:  
<https://ieeexplore.ieee.org/>

# Towards Digitalized and Automated Substations: Implementation of Adaptive Protection Control Unit and Monitoring System for Modern Distribution Networks Under Increased Hosting Capacity of Distributed Renewable Sources

*Ayatte I. Atteya<sup>1,2\*</sup>, Amany El-Zonkoly<sup>2</sup>, Hamdy A. Ashour<sup>2</sup>, Dallia Ali<sup>1</sup>*

*<sup>1</sup>School of Engineering, Robert Gordon University, Aberdeen, Scotland, UK*

*<sup>2</sup>Department of Electrical and Control Engineering, College of Engineering and Technology, Arab Academy for Science, Technology and Maritime Transport, Abu Qir campus, Alexandria, Egypt*

*\*a.atteya@rgu.ac.uk*

**Keywords:** Adaptive Protection Control Unit, Distributed Generation, Monitoring System, Human Machine Interface, Real-time response

## Abstract

Maximizing the hosting capacity of modern distribution networks to accommodate more distributed renewable sources is key driver to realise energy system security and Net-Zero carbon goals. Protection systems under increased share of renewable sources became more challenging with diverse topology changes originated from the addition, disconnection, or islanding of distributed generation to secure increasing energy demands. This paper aims to implement an adaptive protection control unit interlinked with an interactive monitoring system to enable the real-world application of smart adaptive protection schemes for modern distribution networks under increased hosting capacity of distributed renewable sources. An adaptive protection control kit is experimentally developed to enable the automatic adjustment of optimal relay settings in response to network topology changes arising from the integration of distributed generation. A set of relay settings are pre-optimized within a small-scale meshed network under possible network topologies and stored offline via a master microcontroller which then uses the online breaker status to identify the corresponding network topology and accordingly adjust the pre-optimized relay settings. A human machine interface is further designed and interlinked with the experimentally developed control kit via a slave microcontroller, providing real-time data of actual current measurements and waveforms together with topological changes and self-adaptation of pre-optimized relay settings. Experimental results showed successful adjustment of pre-optimized relay settings in response to topological changes while achieving coordination time intervals within acceptable limits under the tested network topologies.

## 1 Introduction

The energy transition plays an increasingly important role in triggering the shift towards more localized renewable potential [1]. Operation and planning of distribution networks under increased hosting capacity of distributed renewable sources are facing considerable challenges, requiring new practices and more modern technologies to ensure safe, reliable, and secure power system operation. Protection under increased electrification is of greatest interest with diverse network topology changes altering the fault current levels further requiring modernized protection systems to dynamically perform relay recalibration to avoid miscoordination of protective devices [2]. This concept is referred as ‘Adaptive Protection Scheme’ and requires key digital advancements in power systems’ operation and planning including automatic control, communication protocols, and monitoring systems [3,4]. This paper addresses these aspects by implementing a smart adaptive protection control unit and monitoring system for modern distribution networks under increased hosting capacity of

distributed renewable sources, towards fostering the automation and digitization of distribution substations. This research work has been conducted on two phases. Phase-1, published in [5], was targeting the operational simulation phase of the adaptive protection scheme by developing a simulation platform interlinking the operation of adaptive protection scheme with the optimization process of relay settings in response to dynamic changes of network topologies. Phase-2, which is presented in this paper, extends the previous work to investigate the implementation of the adaptive protection control unit for enabling its real-world application within modern distribution networks. An experimental set-up is developed to provide a complete testbed for the implementation of the adaptive protection control unit. To enable implementing the adaptive control system, a small-scale three-bus ring network is developed in the power system laboratory to study the real-time response of the implemented adaptive protection control scheme. Pre-optimized relay settings are stored and sent offline to an Arduino Master microcontroller that uses the online breaker status to identify the network topology, and

accordingly adjust the optimum relay settings in response to topological changes. A Human Machine Interface (HMI) is fully integrated with the implemented adaptive protection control unit via a secondary Slave Arduino microcontroller providing a complete supervision and monitoring system to observe dynamic changes of network topologies, real-time data of actual current measurements and self-adaptation of relay settings.

## 2 Motivation

Throughout the years, several researchers have carried out valuable insights to develop adaptive protection schemes based on effective optimization algorithms [6–10]. It has been noticed that research in this area was focused on minimizing the relay trip times in response to topological changes using advanced artificial intelligence algorithms. However, less interest has been given to the real-time simulation of adaptive protection control strategy to enable the automatic adjustment of optimized relay settings. In distribution substations, the dynamic response is of extreme importance when assessing the technical feasibility of introducing new technologies like adaptive protection schemes within existing grid infrastructures. In addition, grid operators will need cutting-edge digital solutions to monitor every single change in networks operation and manage the larger uptake of renewables into the electricity grid. This therefore necessitates coupling the automatic control of distribution substations with the supervisory control of such systems to ensure power system reliability and energy system security. To address this research gap, this paper will implement a fully integrated adaptive protection control and monitoring system to enable observing the real-time response of adaptive protection control schemes towards their real-world application within modern distribution systems. To build-up on the operational simulation platform developed in [5], the same three-bus ring network that was previously considered has been used in this research to observe the real-time response of the implemented adaptive protection control unit. Further data analysis is conducted to validate the simulation results with real-time experimental results obtained by the authors of this research. This experimental validation is key driver in assessing the feasibility of the pre-developed operational simulation platform to be used as a powerful tool for power system developers to emulate the anticipated performance of adaptive protection control systems, further saving time and efforts.

## 3 Case Study

To allow investigating the real-time response of adaptive protection control schemes, a small-scale three-bus ring network was developed in the power system laboratory of the Arab Academy for Science, Technology and Maritime Transport. The network under investigation is of meshed structure, fed from two generation sources acting as the main grid with an additional distributed generation (DG)

source as shown in Fig. 1. Four overcurrent relays were used to protect the considered network, referred as  $K_1$ ,  $K_2$ ,  $K_3$  and  $K_4$  as illustrated in Fig. 1. The network is tested under two proposed network topologies: the first one examines the system when only fed from the utility grid while the second tests the system in the presence of the additional DG source in grid-connected mode. A combined MATLAB simulation and optimization platform was used to optimize the relay settings in response to topological changes. Details of relay settings' optimization process can be found in [5]. Table 1 shows the relays' pre-optimized time dial settings (TDSs) under each of the tested network topologies. Table 2 shows the relay trip times obtained using the pre-optimized TDSs for a single-line-to-ground fault applied at busbar 3 ( $F_3$ ) [5]. For fault  $F_3$  under network topology 1,  $K_3$  and  $K_2$  act as primary relays while  $K_1$  acts as the backup relay in case  $K_2$  or  $K_3$  fails to operate. Given that the DG unit is inactive under network topology 1, then  $K_4$  will go out of service in this case. For fault  $F_3$  under network topology 2,  $K_2$  and  $K_3$  act as primary relays while  $K_1$  and  $K_4$  act as backup relays in case  $K_2$  or  $K_3$  fails to operate.

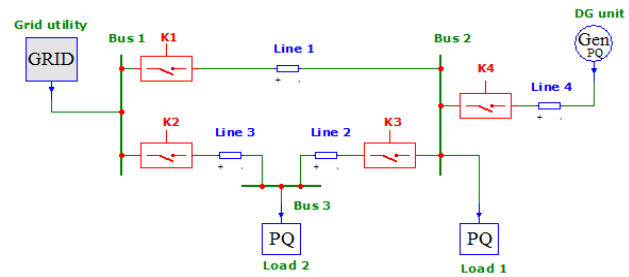


Fig. 1 Single-line diagram of the three-bus ring network

Table 1 Pre-optimized relay TDSs under the tested network topologies

Relay		K1	K2	K3	K4
TDS	Topology 1	0.1	0.1209	0.1	--
	Topology 2	0.1	0.2471	0.17	0.1

Table 2 Relay trip times at fault  $F_3$  under the tested network topologies

Description	Topology 1		Topology 2	
	Relay	Trip time	Relay	Trip time
Primary 1	K3	0.48s	K3	0.88s
Primary 2	K2	0.51s	K2	0.99s
Backup 1	K1	0.91s	K1	1.25s
Backup 2	--		K4	1.496s

### 3 Implementation of Adaptive Protection Control Unit and Monitoring System

An adaptive protection control unit and monitoring system is experimentally developed to study the real-time response of the adaptive protection scheme in responding to network topology changes. Pre-optimized relay settings given in Table 1 are stored into a look-up table for possible network topologies and sent offline to an Arduino microcontroller. The system controller then detects the online breaker status to identify the existing network topology and accordingly adjust the pre-optimized relay settings further performing the anticipated trip actions using controlled actuators. Fig. 2 illustrates the schematic diagram of the implemented adaptive protection control unit and monitoring system. As illustrated in Fig. 2, an experimental setup is developed in the power system laboratory to emulate the network under investigation. The implemented adaptive protection control unit consisted of three-phase contactors acting as motorized circuit breakers to protect the developed network, an Arduino-based primary microcontroller to enable the automatic adjustment of pre-optimized relay settings, and a pre-programmed relay module providing the contactors with the control signals to enable fulfilling the required breaking actions. The control process of adaptive protection scheme can be traced through the inner and outer loops as shown in Fig. 2. In the inner path (blue loop), microcontroller 1 is responsible of gathering two types of data input: the first is the status of installed contactors to identify the network topology, and the second is the actual current measurements continuously acquired to enable detecting any abnormal condition.

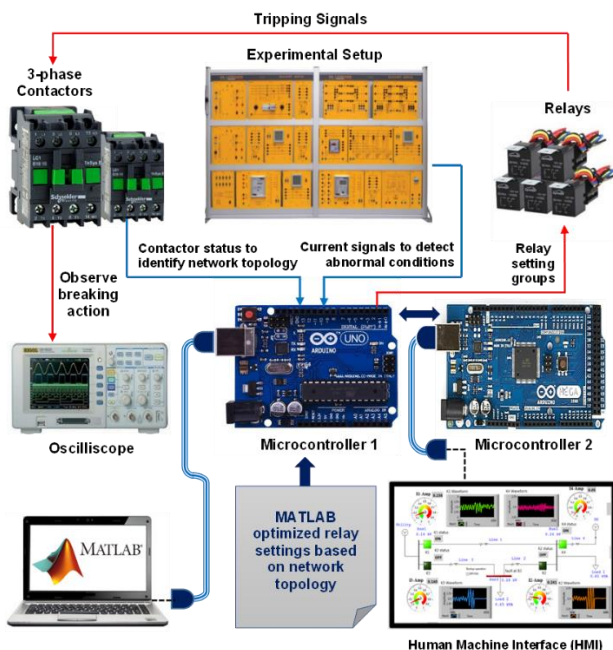


Fig. 2 Schematic diagram of the implemented adaptive protection control unit and monitoring system

The outer path (red loop) shows the track of data output in which microcontroller 1 adjusts the appropriate relay settings based on the identified network topology further allowing the programmed relays to send the tripping signals to the contactors for fulfilling the required action whenever the controller detects the risk of a fault occurrence. During the time of fault, the current signal waveforms are captured and displayed using a visual oscilloscope to observe the real-time response of the implemented adaptive protection approach. An HMI is finally designed and interlinked with the experimentally developed setup via microcontroller 2 to enable monitoring and supervising the implemented adaptive protection control scheme.

### 4 Experimental Set-up

Fig. 3 illustrates the experimental set-up developed for the three-bus ring network. As can be seen from Fig. 3, contactor panels  $K_1$ ,  $K_2$ ,  $K_3$  and  $K_4$  are mounted and connected to feeders 1, 2, 3 and 4 respectively, acting as controlled circuit breakers. It should be noted that contactor  $K_4$  together with feeder 4 are out of service in the absence of DG incoming source under network topology 1. In network topology 2, the additional DG source is injected in grid-connected mode via feeder 4 and synchronised with the main power supply using a synchronizing unit indicator through “bright-dark lamps” method. A voltage, frequency and phase sequence meters are also used to check the two sources are satisfying the necessary conditions for their parallel operation. Fig. 4 illustrates the implemented adaptive protection control kit developed to enable the automatic adjustment of relay settings in response to network topology changes. The developed control kit board mainly consisted of 4 current transformers (CTs) together with the associated signal conditioning circuits to enable measuring the current flowing throughout the 4 feeders and detecting the event of any fault occurrence, a 4-channel relay module interface providing the control trip signals to the 4 contactor panels, 2 microcontrollers to implement and supervise the adaptive control sequence and 4 current meters providing a correct calibration with the CT readings.

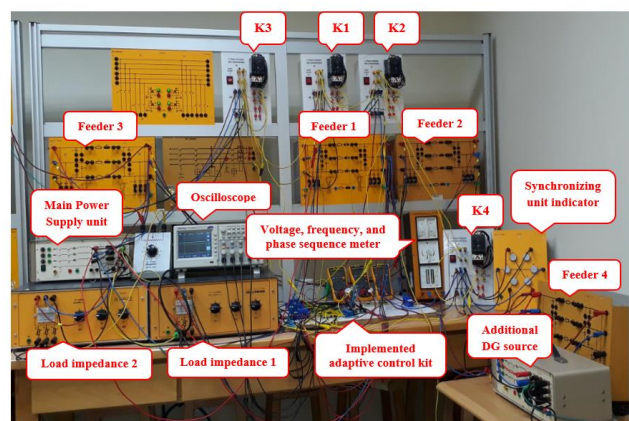


Fig. 3 Experimental setup of the three-bus ring network

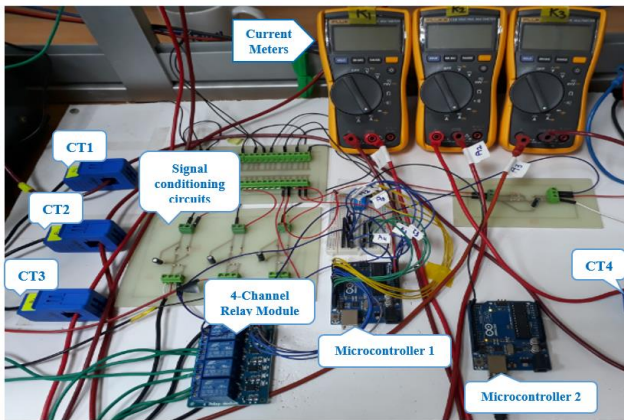


Fig. 4 The implemented adaptive protection control kit board

## 5 Adaptive Protection Control Sequence

The development of the software code for implementing the adaptive protection control system begins by storing the pre-optimized relay settings corresponding to each of the tested network topologies in an offline manner. The user will then start the operation of the contactors using 4 digital input switches connected as digital inputs to microcontroller 1. The latter uses the switch status to identify the network topology, allowing the protection system to adapt itself in response to the existing network topology by configuring the appropriate setting group in an online manner. Along the whole operational process, continuous current measurements are being sent to microcontroller 1 through the CTs which are connected as analog inputs to microcontroller 1, to enable detecting any fault occurrence if either one or more of the measured currents exceeded the pre-specified current setting. Fig. 5 illustrates the overall system inputs and outputs.

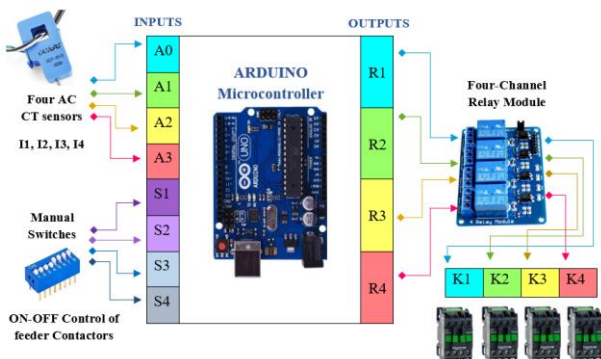


Fig. 5 Overall system inputs and outputs

In case of a fault occurrence, microcontroller 1 identifies the primary and backup relay pairs and accordingly compute their relevant trip times using the configured relay settings belonging to the existing network topology. Breaking actions are taking place through the 4 contactor panels automatically controlled via the 4-channel relay module with the embedded relays representing the digital outputs of

microcontroller 1. Fig. 6 shows the software flowchart of the implemented adaptive protection control sequence.

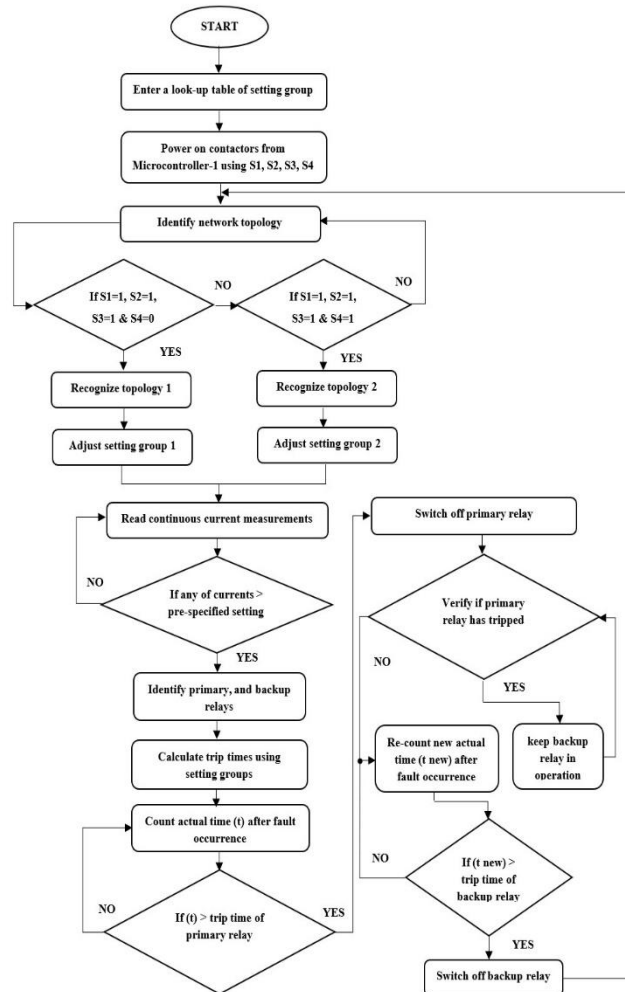


Fig. 6 Software flowchart of the adaptive protection control sequence

## 6 Experimental Results

Fig. 7 shows the experimental primary response of  $K_3$ ,  $K_2$  and  $K_1$  at the time the fault occurred under network topology 1 prior integrating additional DG source. From Fig. 7, it is evident that contactors  $K_3$  and  $K_2$  tripped first disconnecting feeders 2 and 3, while the current passing through contactor  $K_1$  is maintained in operation as the primary relays have satisfactorily isolated the fault. Fig. 8 and Fig. 9 illustrate the experimental trip time responses of primary contactors  $K_3$  and  $K_2$  respectively at the time the fault occurred under network topology 1. The illustrated trip time responses are computed by microcontroller 1 using the pre-optimized TDSs given in Table 1. As can be seen from Fig. 8,  $K_3$  is seen tripping after 488ms while  $K_2$  is seen completely clearing the fault after 536ms as shown in Fig.9. To observe the backup response of the experimentally developed adaptive protection control system, the contactor

$K_2$  has been disconnected from the microcontroller and powered on externally to simulate that it is kept in operation at the time the fault occurred. Fig. 10 shows the experimental backup response of contactors  $K_3$ ,  $K_2$  and  $K_1$  at the time the fault occurred under network topology 1. As can be seen from Fig. 10, when contactor  $K_2$  is kept in operation the backup contactor  $K_1$  is seen completely clearing the fault. Fig. 11 shows the experimental backup trip time sequences of contactors  $K_1$ ,  $K_2$  and  $K_3$  at the time the fault occurred under network topology 1, indicating that backup contactor  $K_1$  has completely cleared the fault after 920ms. To ensure the coordination time interval between contactors  $K_2$  and  $K_1$  is maintained within appropriate margins (no more than 500ms), a virtual trip time signal is illustrated for contactor  $K_2$  when the latter is supposed to appropriately trip the fault, demonstrating a coordination interval of 380ms between  $K_1$  and  $K_2$  as depicted in Fig. 11.

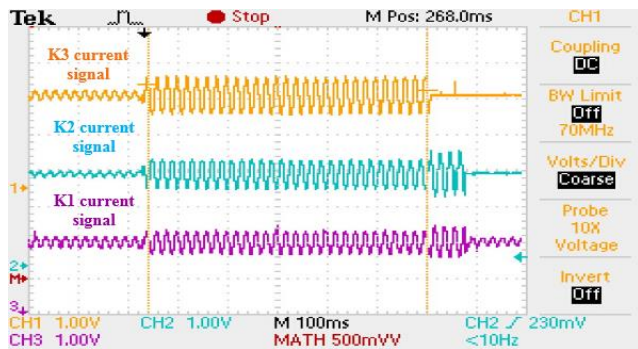


Fig. 7 Experimental primary response of  $K_1$ ,  $K_2$  and  $K_3$  for fault  $F_3$  under network topology 1

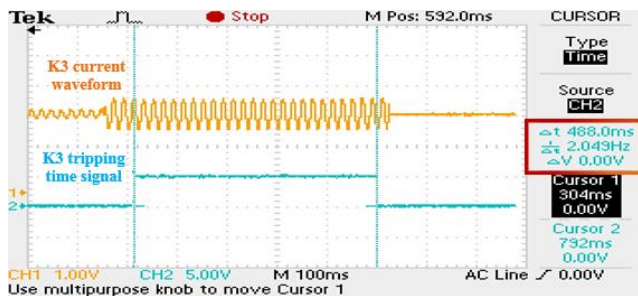


Fig. 8 Experimental primary trip time response of  $K_3$  for fault  $F_3$  under network topology 1

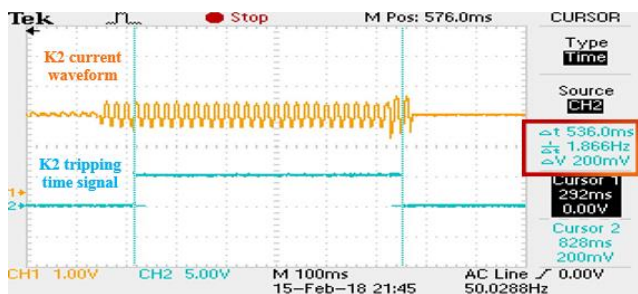


Fig. 9 Experimental primary trip time response of  $K_2$  for fault  $F_3$  under network topology 1

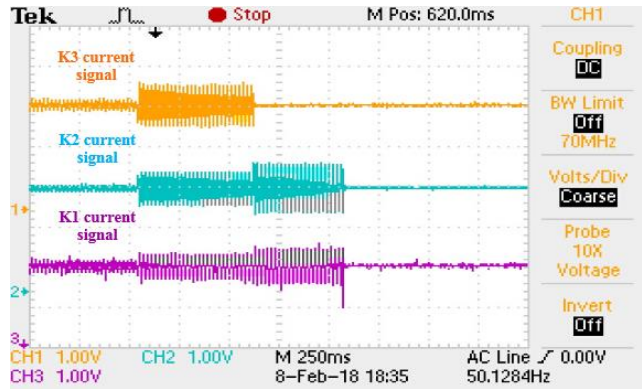


Fig. 10 Experimental backup response of  $K_1$ ,  $K_2$  and  $K_3$  for fault  $F_3$  under network topology 1

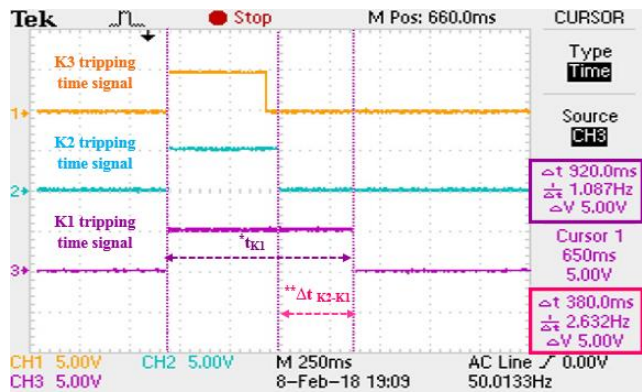


Fig. 11 The experimental backup trip time sequence of  $K_1$ ,  $K_2$  and  $K_3$  for fault  $F_3$  under network topology 1

Fig. 12 shows the experimental primary response of  $K_1$ ,  $K_2$ ,  $K_3$  and  $K_4$  at the time the fault occurred under network topology 2 following the integration of additional DG unit in grid-connected mode through feeder 4. As can be seen from Fig. 12, contactors  $K_2$  and  $K_3$  are seen tripping while the current passing through contactors  $K_1$  and  $K_4$  are kept in operation as the primary relays have satisfactorily cleared the fault. Fig. 13 and Fig. 14 illustrate the experimental trip time responses of primary contactors  $K_3$  and  $K_2$  respectively at the time the fault occurred under network topology 2, showing  $K_3$  is tripping after 880ms while  $K_2$  is completely clearing the fault after 990ms. Compared to network topology 1, it is noticeable that  $K_2$  and  $K_3$  are seen changing relay settings satisfactorily in response to network topology 2, further updating their trip time signals accordingly.

Fig. 15 shows the experimental backup response of contactors  $K_1$ ,  $K_2$ ,  $K_3$  and  $K_4$  at the time the fault occurred under network topology 2. As can be seen from Fig. 15, the current passing through contactor  $K_2$  is kept in operation until being attenuated at the instant the backup contactor  $K_1$  is seen tripping. A few seconds later, the fault current is seen completely cleared by contactor  $K_4$ . Fig. 16 shows the experimental backup trip time sequences of contactors  $K_1$ ,  $K_2$ ,  $K_3$  and  $K_4$  at the time the fault occurred under network topology 2. From Fig. 16, the backup contactor  $K_1$  is seen

achieving a trip time of 1.29s while  $K_4$  is seen achieving a trip time of 1.4s. These results are closely matching with those previously given in Table 2. Fig. 17 illustrates the coordination time intervals achieved between primary contactor  $K_2$  and backup contactors  $K_1$  and  $K_4$ . To enable observing the coordination time intervals achieved, a virtual trip time signal is illustrated for  $K_2$  when it is supposed to work properly to trip the fault. As can be seen from Fig. 17, a coordination interval of 320ms is seen achieved between  $K_1$  and  $K_2$  while a coordination interval of 430ms is seen achieved between  $K_4$  and  $K_2$ , therefore being maintained within acceptable limits for coordination intervals between primary and backup relay pairs (no more than 500ms).

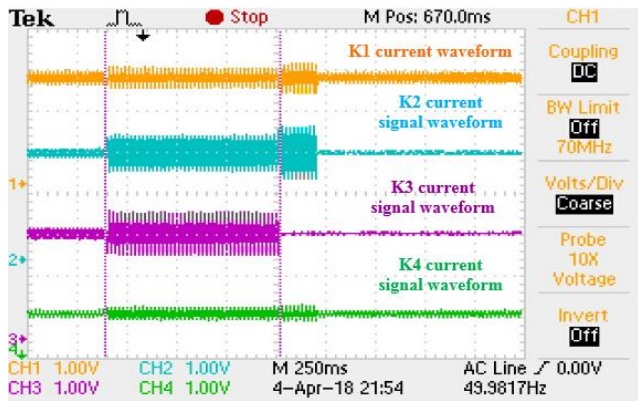


Fig. 12 Experimental primary response of  $K_1$ ,  $K_2$ ,  $K_3$  and  $K_4$  for fault  $F_3$  under network topology 2

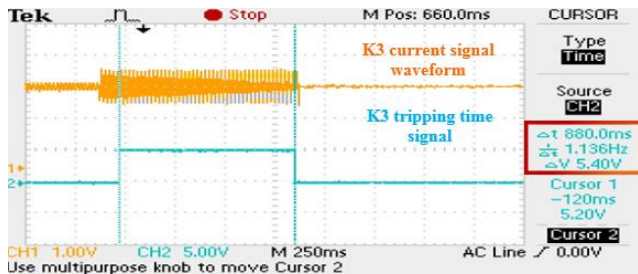


Fig. 13 Experimental primary trip time response of  $K_3$  for fault  $F_3$  under network topology 2

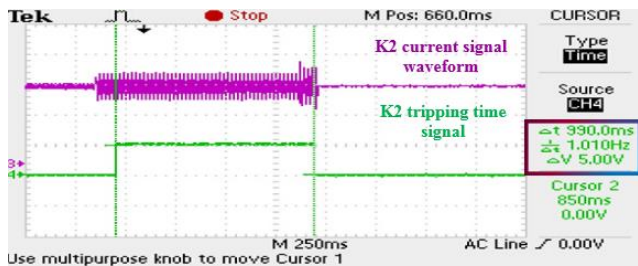


Fig. 14 Experimental primary trip time response of  $K_2$  for fault  $F_3$  under network topology 2

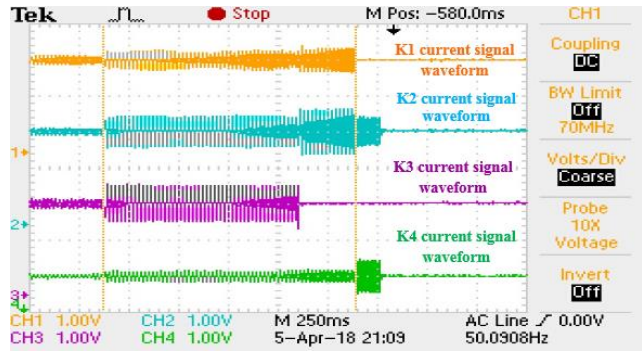


Fig. 15 Experimental backup response of  $K_1$ ,  $K_2$ ,  $K_3$  and  $K_4$  for fault  $F_3$  under network topology 2

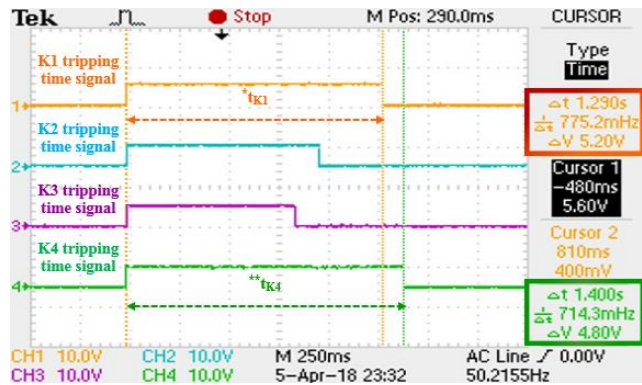


Fig. 16 Experimental backup trip time sequence of  $K_1$ ,  $K_2$ ,  $K_3$  and  $K_4$  for fault  $F_3$  under network topology 2

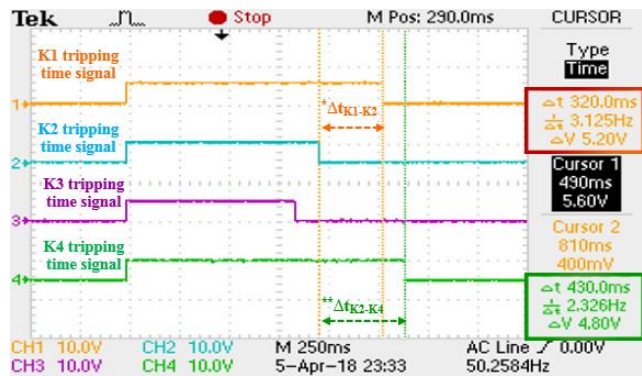


Fig. 17 Experimental results of coordination time intervals achieved for fault  $F_3$  under network topology 2

## 7 Experimental Validation

To enable assessing the technical feasibility of the pre-developed adaptive protection simulation platform in [5], a comparative analysis is held between the simulation results obtained in [5] and the real-time experimental results obtained in this research. Fig. 18 and Fig. 19 compare the results of the pre-developed adaptive protection simulation platform versus those obtained experimentally under network topology 1 and network topology 2, respectively. As can be seen from the comparative analysis, the real-time

experimental results are closely matching with the results obtained from the pre-developed adaptive protection simulation platform with only minor percentage of errors achieved. These errors are due the compiling time taken by the microcontroller to execute the adaptive protection control sequence and the difference between the theoretical load flow analysis conducted by the pre-developed simulation platform and the actual current measurements acquired by the microcontroller. This experimental validation has clearly confirmed the accuracy of the pre-developed adaptive protection simulation platform in [5] in reflecting nearly real-time response analysis of the adaptive protection control scheme towards enabling its real-world application.

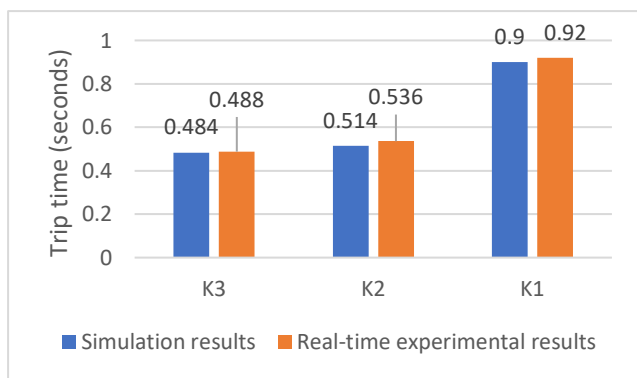


Fig. 18 Comparison between simulation results and real-time experimental results under network topology 1

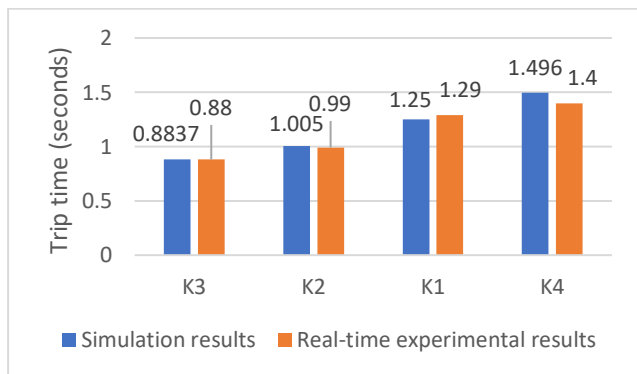


Fig. 19 Comparison between simulation results and real-time experimental results under network topology 2

### 8 The Integrated Monitoring System

An HMI is fully integrated with the implemented adaptive protection control unit via microcontroller 2, providing a graphical user interface (GUI) for grid operators to monitor real-time data of actual current measurements acquired by microcontroller 1 together with self-adaptation of pre-optimized relay settings. The HMI is designed using LabVIEW software and consists of 4 current gauges as shown in Fig. 20, to enable monitoring the real-time current measurements passing through contactors K<sub>1</sub>, K<sub>2</sub>, K<sub>3</sub> and

K<sub>4</sub>. A graphical scope chart is presented beside each current gauge to enable visualizing the current waveform passing through each of the 4 contactors. To ensure accurate monitoring of real-time actual current measurements, the HMI current readings are carefully calibrated with the actual current measurements provided by the current meters of the experimental setup during normal operation before a fault is being applied to busbar 3. On the right-hand side of the designed HMI visualization screen, there is an alarming and notifications section for the user. A red LED alarm is used to notify the user whenever a fault occurs. In addition, a set of tabs are used to display the pre-optimized TDSs corresponding to each network topology to enable monitoring the self-adaptation of relays settings in response to network topology changes. Visualization results of the integrated HMI are captured for fault F<sub>3</sub> under network topology 1 and network topology 2 and displayed in Fig. 20 and Fig. 21 respectively. As can be seen from Fig. 20, the current waveforms passing through contactors K<sub>2</sub> and K<sub>3</sub> are seen interrupted while the current waveform passing through contactor K<sub>1</sub> is kept in operation as experimentally implemented for the primary response of fault F<sub>3</sub> under network topology 1. From Fig. 21, the current waveforms passing through contactors K<sub>2</sub> and K<sub>3</sub> are seen interrupted while the current waveform passing through contactors K<sub>1</sub> and K<sub>4</sub> are kept in operation as experimentally implemented for the primary response of fault F<sub>3</sub> under network topology 2. Change in network topology together with pre-optimized TDSs is noted and monitored accordingly, enabling the user to observe the real-time response of the implemented adaptive protection control system.

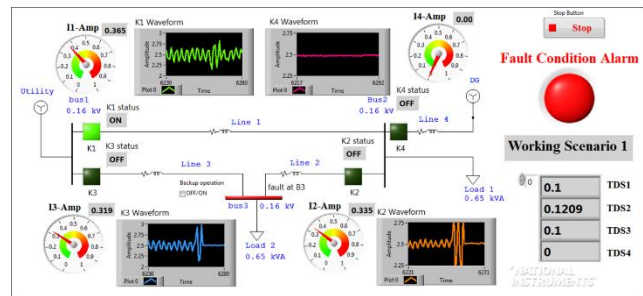


Fig. 20 The designed HMI screen visualisation for fault F<sub>3</sub> under network topology 1

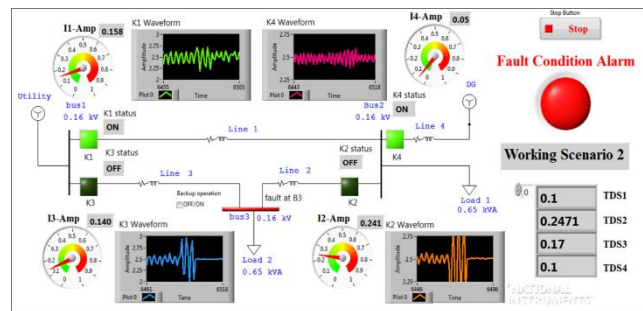


Fig. 21 The designed HMI screen visualisation for fault F<sub>3</sub> under network topology 2



## 9 Conclusion

This paper addressed the implementation of an adaptive protection control and monitoring system for investigating its real-time response within modern distribution networks under increased hosting capacity of distributed generation. An adaptive protection control system is experimentally developed, tested, and validated through a small-scale three-bus network under two proposed network topologies. The implemented adaptive protection control system has proven effectiveness in responding to subjected topology changes achieving successful adjustment of pre-optimized relay settings while maintaining coordination intervals within acceptable limits under each of the tested network topologies. The implemented adaptive protection control system has been also used to experimentally validate the performance of a previously developed adaptive protection simulation platform. It was found that the latter reveals enough accuracy in emulating the real-world performance of adaptive protection schemes and this was confirmed by matching the simulation results with real-time experimental results. An HMI is further integrated with the implemented adaptive protection control system allowing grid operators to observe real-time data of actual current measurements and self-adaptation of relay settings. The application of the implemented adaptive protection control and monitoring system is expected to add key valuable outcomes in terms of operation and control of distribution systems, allowing to mitigate the impact of distributed generation on protection systems while providing the ability to monitor and supervise the real-time response of adaptive protection schemes.

## 10 Acknowledgements

The authors would like to thank the Arab Academy for Science, Technology and Maritime Transport for providing access to its lab facilities to conduct this research work.

## 10 References

- [1] Bp. bp Energy Outlook 2023. <https://www.bp.com/en/global/corporate/energy-economics/energy-outlook.html>.
- [2] Wong J, Tan C, Rahim NA, Tan RHG. A Communication-less adaptive protection scheme for Self-Healing distribution systems. *International Journal of Electrical Power & Energy Systems* 2023;148:108992. <https://doi.org/https://doi.org/10.1016/j.ijepes.2023.108992>.
- [3] Islam K, Kim D, Abu-Siada A. A review on adaptive power system protection schemes for future smart and micro grids, challenges and opportunities. *Electric Power Systems Research* 2024;230:110241. <https://doi.org/https://doi.org/10.1016/j.eprsr.2024.110241>.
- [4] Shobole AA, Abafogi M, Zaim A, Amireh Y. Multi agent system based adaptive numerical relay design and development, Part II: Hardware. *Electric Power Systems Research* 2024;226:109889. <https://doi.org/https://doi.org/10.1016/j.eprsr.2023.109889>.
- [5] Atteya AI, El-Zonkoly A, Ashour HA, Ali D. Developing an Adaptive Protection Scheme Towards Promoting the Deployment of Distributed Renewable Sources in Modern Distribution Networks: Operational Simulation Phase. 2023 58th International Universities Power Engineering Conference (UPEC), 2023, p. 1–6. <https://doi.org/10.1109/UPEC57427.2023.10294344>.
- [6] Abdelhamid M, Kamel S, Ahmed EM, Agyekum EB. An Adaptive Protection Scheme Based on a Modified Heap-Based Optimizer for Distance and Directional Overcurrent Relays Coordination in Distribution Systems. *Mathematics* 2022;10. <https://doi.org/10.3390/math10030419>.
- [7] Abdelhamid M, Kamel S, Korashy A, Tostado-Véliz M, Banakhr FA, Mosaad MI. An adaptive protection scheme for coordination of distance and directional overcurrent relays in distribution systems based on a modified school-based optimizer. *Electronics (Switzerland)* 2021;10. <https://doi.org/10.3390/electronics10212628>.
- [8] Irfan M, Oh SR, Rhee SB. An effective coordination setting for directional overcurrent relays using modified harris hawk optimization. *Electronics (Switzerland)* 2021;10. <https://doi.org/10.3390/electronics10233007>.
- [9] Irfan M, Wadood A, Khurshaid T, Khan BM, Kim KC, Oh SR, et al. An optimized adaptive protection scheme for numerical and directional overcurrent relay coordination using harris hawk optimization. *Energies (Basel)* 2021;14. <https://doi.org/10.3390/en14185603>.
- [10] Alam MN. Adaptive Protection Coordination Scheme Using Numerical Directional Overcurrent Relays. *IEEE Trans Industr Inform* 2019;15:64–73. <https://doi.org/10.1109/TII.2018.2834474>.